

SSR mitigation in power system with static synchronous series compensator

Nilaykumar A. Patel ^{1*}, Dr. Praghnes Bhatt ¹

¹ Chandubhai S. Patel Institute of Technology, CHARUSAT, Changa

*Corresponding author E-mail: nilaypatel.cem@charusat.ac.in

Abstract

Series compensation in transmission line with fixed series capacitor may cause Subsynchronous Resonance (SSR) at certain compensation level. This paper presents the application of static synchronous series compensator (SSSC) to mitigate impact of SSR. For analysis of SSR, IEEE first benchmark model is used and SSSC is located in transmission line at generator end. The linearized state space equation of SMIB system without and with SSSC has been developed to carry out eigenvalue analysis to identify potential modes for SSR. The AVR and PSS in the generator control loop coordinated with SSSC can successfully mitigate SSR. Time domain simulation is also carried out to confirm the results obtained with eigenvalue analysis.

Keywords: Subsynchronous Resonance; Simulation; Eigenvalues; Static Synchronous Series Compensator.

1. Introduction

Series compensation of transmission line with fixed series capacitors has been used widely in long power transmission systems for enhancing power transfer capability and improving different stability limits [1]. But the different power system components such as generators, transformers, transmission lines and series capacitors experience an electrical resonance when series compensation reaches to a certain level [2-3].

In thermal power plants, the components of turbo-generator such as synchronous generator, different pressure stages of turbine are connected through different shaft sections which have been modeled as torsional springs with different stiffness coefficient depending upon shaft section diameter. Hence, such spring-mass model of turbo-generator has several modes of oscillations, known as torsional modes, when resonant frequency of electrical network becomes complementary to one of the torsional frequencies of turbo-generator mechanical system. This will result in either undamped or unstable oscillations which may endanger the turbo-generator and this phenomena is known as SSR [4-6].

The emergence of Flexible AC Transmission Systems (FACTS) has improved the steady state and dynamic performance of power system to a great extent. FACTS devices can control power flow in interconnected power system which may provide a number of benefits such as prevention of unwanted loop flows; transfer a power over intended path; enhancing transfer capability of line pushing towards their thermal limits [7-8]. In [9], small signal performance of the power system has been shown to be improved by controlling

the damping characteristic of power system by controlling the operation mode and response time of FACTS controller. Hence, taking this advantage of FACTS controller, their capability to influence SSR mitigation has been assessed in [10].

This paper investigates the capability of SSSC to mitigate SSR. The mathematical model of IEEE FBM with synchronous generator model 2.2 equipped with AVR and PSS has been developed. The linearized state space equations have been formulated to carry out eigenvalue analysis along with SSSC to demonstrate their dynamic characteristic to control torsional modes of oscillations.

2. Analysis of SSR for IEEE FBM

IEEE First Benchmark Model (FBM) shown in Fig. 1 is adopted for SSR analysis [4]. The turbo-generator rated at 892.4 MVA is connected to 500 kV long transmission line through a step up transformer. The reactance of this transformer is denoted as X_T . The impedance of the line is represented by $R + jX_L$ whereas there are two options for series compensation. In case one, the series compensation is considered with fixed series capacitor and in other case fixed series capacitors are replaced with SSSC. The connecting reactance between transmission network and infinite bus is represented by X_{SYS} . The mechanical system of turbo-generator is represented by six lumped masses: a high pressure turbine (HP), an intermediate pressure turbine (IP), two low pressure turbines (LPA, LPB), the generator (GEN) and the exciter (EXC). These rotating masses are mechanically coupled by soft shaft sections. The parameters of the system shown in Fig. 1 are given in Appendix.

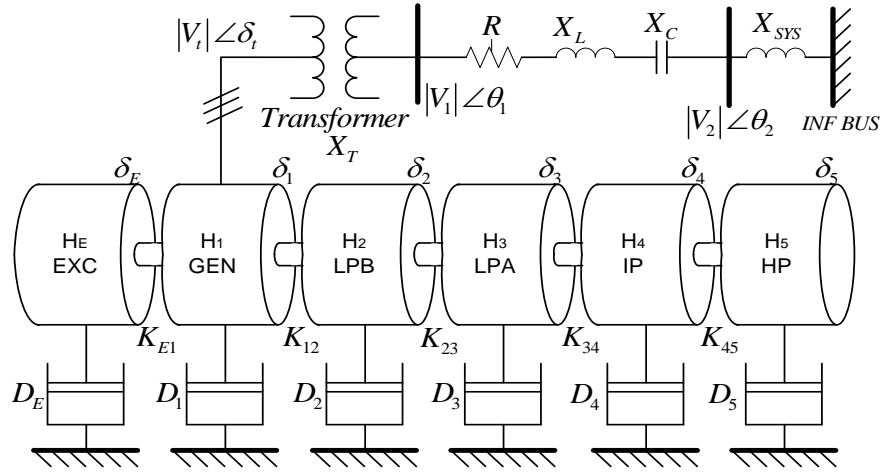


Fig. 1: IEEE FBM for SSR Study.

2.1. Synchronous generator modeling

The synchronous generator model is derived from [11] based on the usual assumptions relevant to the two-axis theory and state space equations are derived in terms of flux linkages. The synchronous generator is modeled by taking one damper winding (k_d) on d-axis along with its usual field winding (f_d) and two damper windings on q-axis (k_{q1} , k_{q2}). The notations used in (1) are well described in Appendix.

$$\frac{d}{dt} x_e = [A_e] x_e + [B_{ev}] \begin{bmatrix} V_{q1} \\ V_{q2} \\ \Delta e_{afd} \\ \Delta V_{kd} \end{bmatrix} + [B_{ef}] \begin{bmatrix} \Delta V_{kq1} \\ \Delta V_{kq2} \\ \Delta e_{afd} \\ \Delta V_{kd} \end{bmatrix} \quad (1)$$

Air gap electrical torque equation is given by (2)

$$T_e = \psi_{ds} i_{qs} - \psi_{qs} i_{ds} \quad (2)$$

2.2. Shaft equations modeling

The turbine-generator mechanical system shown in Fig. 1 is represented by four stages of turbine, one stage of generator and exciter each. These six masses of different inertias are interconnected by

five soft steel shafts and can be represented by following shaft torque equations given in (3).

$$[2H] p^2 \delta + [D] p \delta + [K] \delta + T = 0 \quad (3)$$

Where [H] and [D] are diagonal matrix of inertias and damping coefficients, respectively, and [K] is shaft stiffness matrix. T gives torque vector acting on the shaft end and δ us the resulting angular position vector. The inertia constants, damping coefficient and shaft stiffness of different stages are given in Appendix. In this paper damping is ignored.

2.3. Excitation system and PSS modeling

Automatic voltage regulator restores the terminal voltage of alternator during normal conditions as well as during disturbances. The gain K_A is set high for the faster restoration of terminal voltage in the event of disturbance which ultimately results in negative damping torque. The effect of this negative damping torque may lead the system in oscillatory unstable mode under certain operating conditions. The countermeasure to overcome this adverse impact of fast reacting AVR, the synchronous generator is equipped with power system stabilizer (PSS) which can stabilize the system in wider operating range. The combined block diagram for AVR and PSS is presented in Fig. 2.

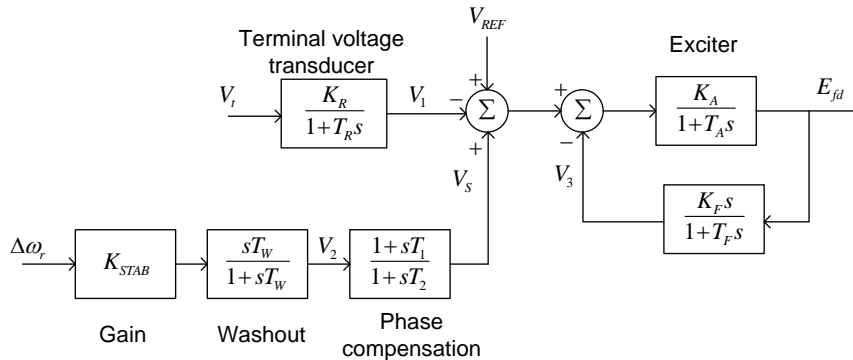


Fig. 2: AVR and PSS Block Diagram.

The dynamic equations for AVR and PSS are given by set of equations in (4) and (5), respectively. The parameters of matrices are given in Appendix.

$$\frac{d}{dt} x_{av} = [A_{av}] x_{av} + \frac{K_R}{T_R} V_t + [B_{avv}] [I_{pss}] x_{pss} + [B_{avt}] v_{ref} \quad (4)$$

$$\frac{d}{dt} x_{pss} = [A_{pss}] x_{pss} + [B_{pss}] [I_{av}] x_m \quad (5)$$

2.4. Network interfacing

Fig. 3 represents the electrical representation of IEEE FBM where transmission line is represented with lumped parameters. The terminal of the generator is connected to infinite bus through these lumped parameters of transmission line which is shown to be compensated by fixed series capacitor. In the analysis, series compensation level is considered to be 50% which comes to 0.371 pu of

series capacitive reactance. Terminal voltage of the generator is represented in (5) using d-q transformation along with the transient voltage developed across the capacitor.

$$\left. \begin{aligned} v_{sd} &= Ri_d + L \frac{d}{dt} i_d - \omega L i_q + v_{cd} + v_{\infty d} \\ v_{sq} &= Ri_q + L \frac{d}{dt} i_q + \omega L i_d + v_{cq} + v_{\infty q} \\ \frac{d}{dt} v_{cd} &= \omega v_{cq} + \frac{1}{C} i_d \\ \frac{d}{dt} v_{cq} &= -\omega v_{cd} + \frac{1}{C} i_q \end{aligned} \right\} \quad (5)$$

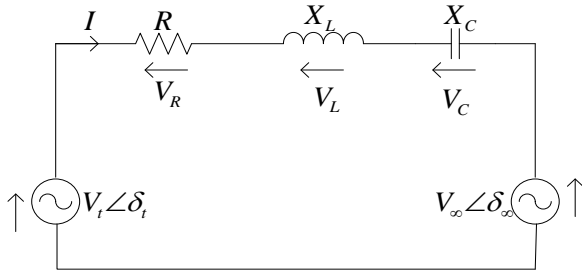


Fig. 3: Representation of IEEE FBM with Network Interfacing.

3. SSSC modeling

In Fig. 1, the active power transfer between bus 1 and bus 2 can be expressed in approximate form after ignoring the resistance of line by

$$P_{12} \approx \frac{|V_1||V_2|}{X_L - X_{SSSC}} \sin \theta_{12} \quad (6)$$

Where $|V_1|$ and $|V_2|$ are voltage magnitudes of bus 1 and bus 2, θ_{12} is the transmission angle between these two bus voltages. The concepts of controlling active power flow between two buses with series compensation can be better explained by (6). In (6), two modes of operation for SSSC can be observed, namely ‘‘constant angle strategy’’ and ‘‘constant power strategy’’. The active power transfer for a given constant transmission angle δ_{12} can be increased by reducing the net reactance $X_L - X_{SSSC}$. This can be accomplished by increasing the controllable compensation level of SSSC. In constant power strategy, compensation level can be changed for reducing the transmission angle needed for constant active power flow in a given line. In this paper, constant angle strategy is adopted.

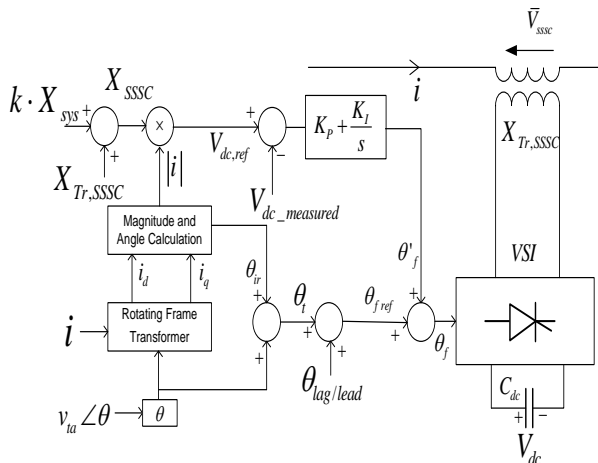


Fig. 4: (a) Schematic Block Diagram for SSSC Control.

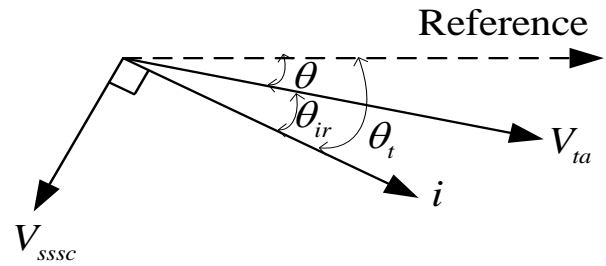


Fig. 4: (b) Phasor Relation with SSSC.

Fig. 4 shows the block diagram of an SSSC and its main controls. A voltage-sourced inverter (VSI) and a coupling transformer are the main parts of SSSC. VSI of SSSC injects ac output voltage in series with transmission line. The control scheme of the SSSC as shown in Fig. 4 is based on constant angle strategy where SSSC compensate the required equivalent voltage demanded by the change in power through the transmission line in normal as well as in any transient condition. Independent control of magnitude and phase angle of equivalent compensating voltage can be possible at the output of VSI terminal. Compensating voltage magnitude can be estimated by multiplying magnitude of line current and commanded reactance value of SSSC as shown in Fig. 4. Similarly, phase angle control for compensating voltage requires setting of $\theta_{lag/lead}$. To get fully capacitive compensation, θ_{lag} is set to -90° and it is set to $+90^\circ$ to obtain full inductive compensation. In Fig. 4 (a), k is the percentage compensation level. For these two phase angle of $\theta_{f,ref}$, SSSC will not exchange any active power and will be responsible for controlling only reactive power. The state space equation for SSSC is given in (7).

$$\frac{d}{dt} \begin{bmatrix} i_q \\ i_d \\ V_{dc} \end{bmatrix} = [L_{SSSC}] \begin{bmatrix} i_q \\ i_d \\ V_{dc} \end{bmatrix} + \frac{1}{L_s} \begin{bmatrix} v_{sq} \\ v_{sd} \\ v_{dc} \end{bmatrix} - \frac{1}{L_s} \begin{bmatrix} v_{sq} \\ v_{sd} \\ v_{dc} \end{bmatrix} \quad (7)$$

Where

$$L_{SSSC} = \begin{bmatrix} -\frac{R_s}{L_s} & -\omega & -\frac{m}{2L_s} \cos \theta_f \\ \omega & -\frac{R_s}{L_s} & \frac{m}{2L_s} \sin \theta_f \\ \frac{3m}{4C_{dc}} \cos \theta_f & -\frac{3m}{4C_{dc}} \sin \theta_f & -\frac{1}{R_{dc} C_{dc}} \end{bmatrix}$$

4. Simulation results and discussions

Simulation of the work have been carried out using MATLAB/SIMULINK. Simulation results of SSR analysis of the test system shown in Fig. 1 is presented in this section. The line is compensated by 50%, i.e. k in Fig. 4 (a) is set to 50%. Following three different case studies have been adopted for SSR analysis. For all the cases, both eigenvalue analysis and time domain simulations have been carried out to explain the SSR characteristic.

Case 1: System with fixed series capacitors; equations (1)-(3), (5) are used for [A] matrix

Case 2: System with SSSC; equations (1)-(3), (7) are used for [A] matrix

Case 3: System with SSSC coordinated with AVR+PSS at generator; equations (1)-(5), (7) are used for [A] matrix

Table 1 shows the eigenvalue results of SSR analysis where the comparison between different cases are presented. The objectives are to identify critical modes of oscillation which are responsible to force the system in state of SSR. The multi mass turbine-generator set has its own oscillating natural frequencies. When series compensation level of 50% is applied in the network, the natural fre-

quency of oscillation of electrical network exactly matches with frequency of torsional mode 1. So when the system will experience any kind of disturbance, then it will become unstable through this mode leading to damage of shaft. Fig. 5 shows the time domain response of oscillations of masses and the shaft torque between LPA

and LPB turbine for the disturbance applied at $t = 10$ Sec. It can be clearly seen from Fig. 5 and results tabulated in Table 1 that the frequency of oscillations exactly match with each other.

Table 1: Eigenvalue Analysis of IEEE FBM for Different Cases

Case I IEEE FBM with 50% series compensation	Case II IEEE FBM 50% series compensation is replaced by SSSC	Case III IEEE FBM SSSC+AVR-PSS	Modes of Oscillations
$-0.00 \pm 297.97i$	$-0.181 \pm 297.97i$	$-0.002 \pm 297.97i$	Torsional mechanical mode #5
$-0.00021 \pm 202.84i$	$-0.025 \pm 202.91i$	$-0.008 \pm 202.88i$	Torsional mechanical mode #4
$-0.00036 \pm 160.50i$	$-0.151 \pm 160.53i$	$-0.0059 \pm 160.51i$	Torsional mechanical mode #3
$0.0004 \pm 126.94i$	$-0.65 \pm 126.95i$	$-0.0022 \pm 126.95i$	Torsional mechanical mode #2
$0.001 \pm 98.70i$	$-0.016 \pm 98.77i$	$-0.039 \pm 98.71i$	Torsional mechanical mode #1
0.00135	$1.179 \pm 12.12i$	$-0.001 \pm 12.13i$	Swing Mode
$-2.636 \pm 130.35i$	$-10.00 \pm 47.06i$	$-3.89 \pm 39.58i$	Subsynchronous Mode
$-4.716 \pm 623.63i$	$-118.218 \pm 547.17i$	$-84.56 \pm 733.75i$	Supersynchronous mode
-0.00	$-3.47 \pm 0.77i$	$-0.64 \pm 0.77i$	
$-0.998, -4.4399$	$-20.509, -32.808$	$-2.763 \pm 1.81i$	Other modes
$-20.467, -33.194$		$-20.470, -24.055$	
		$-35.690, -100.452$	
		-494.272	

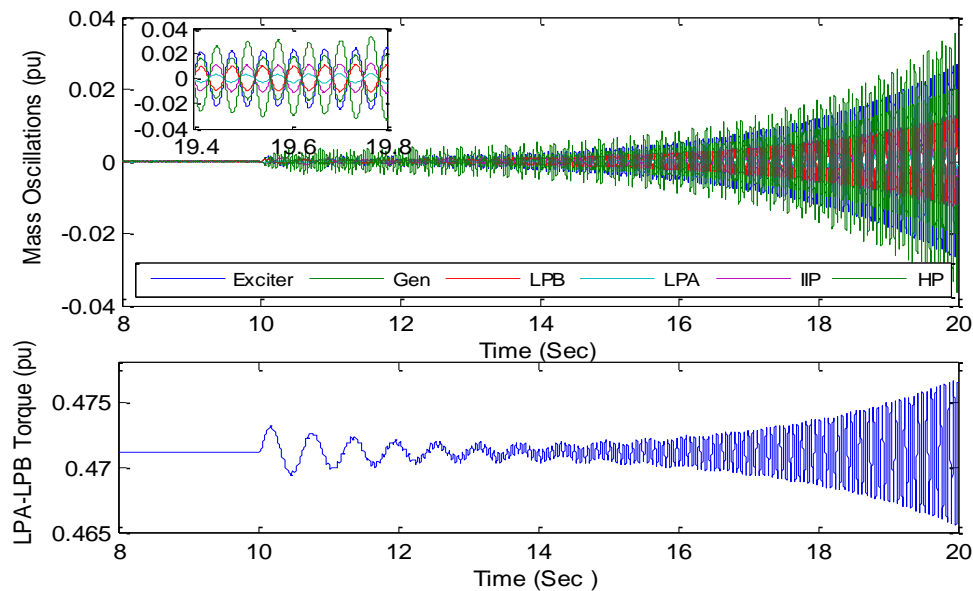


Fig. 5: Oscillations of Masses and LPA-LPB Shaft Torque for Case 1.

To stabilize the system, the approach of applying series compensation by fixed series capacitors has been modified and application of SSSC has been explored to evaluate its impact on SSR behavior of the system. The results of eigenvalue analysis of the system after incorporating SSSC have revealed that SSSC can successfully damp out the torsional modes of oscillations. Also, the application of SSSC increases distance of poles from the $j\omega$ axis towards left hand side which is an indication of addition of more damping for all torsional modes. Even though SSSC increases the damping for torsional modes, it is failed to stabilize the swing mode and system becomes again sustain oscillatory unstable which is shown in fig. 6. In this analysis, the damping of mechanical system is considered as zero, this is the reason of low magnitude sustain oscillation.

In order to completely suppress the oscillation, the coordination of PSS at the generator and SSSC has been proposed to achieve the stable operation of system. This coordinated operation of PSS and SSSC can successfully damped all oscillating modes and make the system stable. The dynamic responses shown in fig 7 further confirms the results obtained with eigenvalue analysis and gives the indication that the system can be operated with 50% series compensation applied with SSSC provided the generator is equipped with PSS.

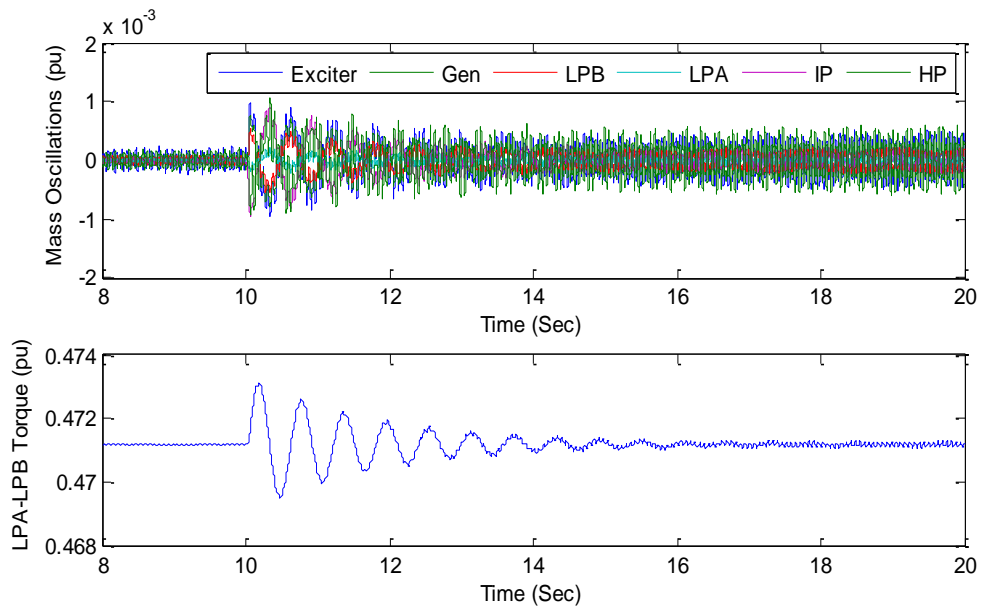


Fig. 6: Oscillations of Masses and LPA-LPB Shaft Torque for Case 2.

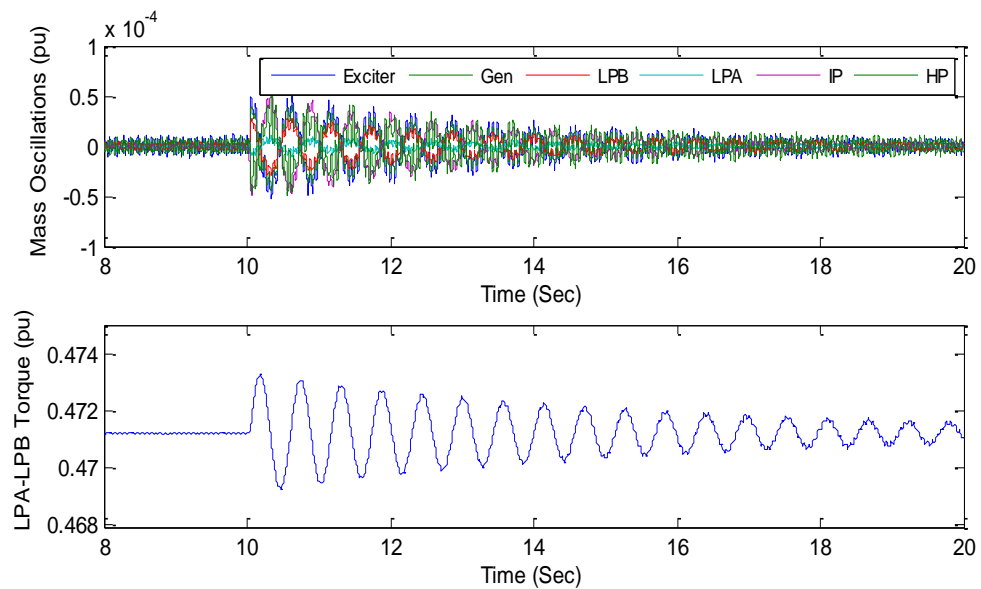


Fig. 7: Oscillations of Masses and LPA-LPB Shaft Torque for Case 3.

5. Conclusion

In this paper, comprehensive modeling of IEEE FBM for SSR analysis is presented. The detailed model of synchronous generator with 2.2 model equipped with AVR and PSS are interfaced with series compensated network for formulating linearized state space equations. SSSC is modeled with constant angle strategy to have the benefit of series compensation and to mitigate SSR. The eigenvalue

analysis with coordinated operation of SSSC with AVR and PSS can successfully mitigate the adverse impact of SSR and stabilized the system.

6. Appendix

Parameters for Turbine-Generator

Reactance (pu)	Time Constant (sec)	Inertia Constant (H) (MW-s/MVA)	Spring Constant (K) in pu torque/rad	
Xd	T'_{d0}	4.3	HP-IP	19.303
X'd	T''_{d0}	0.032	IP turbine	34.929
X''d	T'_{d0}	0.85	LPA turbine	52.038
Xq	T''_{q0}	0.05	LPB turbine	70.858
X'q			Generator	2.82
X''q			Exciter	
Xad				

Elements of Equation (1) are given in (A.1)-(A.4).

$$[A_c] = \begin{bmatrix} \frac{r_s \omega_b}{x_{ls}} \left(\frac{x_{aq} - 1}{x_{ls}} \right) & 0 & \frac{r_s \omega_b}{x_{ls}} \left(\frac{x_{aq}}{x_{lkq1}} \right) & \frac{r_s \omega_b}{x_{ls}} \left(\frac{x_{aq}}{x_{lkq2}} \right) & 0 & 0 \\ 0 & \frac{r_s \omega_b}{x_{ls}} \left(\frac{x_{ad} - 1}{x_{ls}} \right) & 0 & 0 & \frac{r_s \omega_b}{x_{ls}} \left(\frac{x_{ad}}{x_{lfd}} \right) & \frac{r_s \omega_b}{x_{ls}} \left(\frac{x_{ad}}{x_{lkd}} \right) \\ \frac{r_{lkq1} \omega_b}{x_{lkq1}} \left(\frac{x_{aq}}{x_{ls}} \right) & 0 & \frac{r_{lkq1} \omega_b}{x_{lkq1}} \left(\frac{x_{aq} - 1}{x_{lkq1}} \right) & \frac{r_{lkq1} \omega_b}{x_{lkq1}} \left(\frac{x_{aq}}{x_{lkq2}} \right) & 0 & 0 \\ \frac{r_{lkq2} \omega_b}{x_{lkq2}} \left(\frac{x_{aq}}{x_{ls}} \right) & 0 & \frac{r_{lkq2} \omega_b}{x_{lkq2}} \left(\frac{x_{aq}}{x_{lkq1}} \right) & \frac{r_{lkq2} \omega_b}{x_{lkq2}} \left(\frac{x_{aq} - 1}{x_{lkq2}} \right) & 0 & 0 \\ 0 & \frac{r_{lfd} \omega_b}{x_{lfd}} \left(\frac{x_{ad}}{x_{ls}} \right) & 0 & 0 & \frac{r_{lfd} \omega_b}{x_{lfd}} \left(\frac{x_{ad} - 1}{x_{lfd}} \right) & \frac{r_{lfd} \omega_b}{x_{lfd}} \left(\frac{x_{ad}}{x_{lkd}} \right) \\ 0 & \frac{r_{lkd} \omega_b}{x_{lkd}} \left(\frac{x_{ad}}{x_{ls}} \right) & 0 & 0 & \frac{r_{lkd} \omega_b}{x_{lkd}} \left(\frac{x_{ad}}{x_{lfd}} \right) & \frac{r_{lkd} \omega_b}{x_{lkd}} \left(\frac{x_{ad} - 1}{x_{lkd}} \right) \end{bmatrix} \quad (A.1)$$

$$x_c = [\psi_{qs} \quad \psi_{ds} \quad \psi_{kq1} \quad \psi_{kq2} \quad \psi_{fd} \quad \psi_{kd}]^T \quad (A.2)$$

$$B_{cN} = \begin{bmatrix} \omega_b & 0 & 0 & 0 & 0 & 0 \\ 0 & \omega_b & 0 & 0 & 0 & 0 \end{bmatrix}^T \quad (A.3)$$

$$B_{cP} = \begin{bmatrix} 0 & 0 & 0 & 0 \\ 0 & 0 & 0 & 0 \\ \omega_b & 0 & 0 & 0 \\ 0 & \omega_b & 0 & 0 \\ 0 & 0 & \frac{\omega_b r_{lfd}}{x_{md}} & 0 \\ 0 & 0 & 0 & \omega_b \end{bmatrix} \quad (A.4)$$

Elements of Equation (4) are given in (A.5)-(A.8)

$$x_{cs} = [v_1 \quad v_3 \quad e_{fd}]^T \quad (A.5)$$

$$[A_{cs}] = \begin{bmatrix} -\frac{1}{T_R} & 0 & 0 \\ -\frac{K_f K_A}{T_f T_A} & -\frac{1}{T_f} \left(\frac{K_f K_A}{T_A} + 1 \right) & -\frac{K_f}{T_f T_A} \\ -\frac{K_f}{T_A} & -\frac{K_A}{T_A} & -\frac{1}{T_A} \end{bmatrix} \quad (A.6)$$

$$[B_{csT1}] = \begin{bmatrix} 0 & \frac{K_f K_A}{T_f T_A} & \frac{K_A}{T_A} \end{bmatrix}^T \quad (A.7)$$

$$[I_{ps}] = [0 \quad 1] \quad (A.8)$$

Elements of Equation (5) are given in (A.9)-(A.13)

$$[A_{ps}] = \begin{bmatrix} -\frac{1}{T_w} & 0 \\ \frac{T_1}{T_2 T_w} + \frac{1}{T_2} & -\frac{1}{T_2} \end{bmatrix} \quad (A.9)$$

$$[B_{ps}] = \begin{bmatrix} K_{STAB} & \frac{T_1}{T_2} K_{STAB} \end{bmatrix}^T \quad (A.10)$$

$$[I_w] = [0 \quad 1 \quad 0 \quad 0 \quad 0 \quad 0 \quad 0 \quad 0 \quad 0 \quad 0 \quad 0] \quad (A.11)$$

$$x_m = [\omega_E \quad \omega_1 \quad \omega_2 \quad \omega_3 \quad \omega_4 \quad \omega_5 \quad \delta_E \quad \delta_1 \quad \delta_2 \quad \delta_3 \quad \delta_4 \quad \delta_5]^T \quad (A.12)$$

$$x_{ps} = [v_2 \quad v_3]^T \quad (A.13)$$

References

- [1] Marhur R M, Verma R K. Thyristor-based FACTS controllers for electrical transmission systems. New York, USA: IEEE Press and Wiley Inter science; 2002.
- [2] IEEE Subsynchronous resonance Task Force. "First benchmark model for computer simulation of subsynchronous resonance". IEEE transaction on power apparatus and systems, vol. PAS 96, no. 5, pp. 1565-72, 1977.
- [3] IEEE subsynchronous Resonance Working Group, "Terms, definitions and symbol for Subsynchronous oscillations". In: IEEE Trans power apparatus and systems, vol. PAS-104 (6), pp. 1326-1334, 1985. <https://doi.org/10.1109/TPAS.1985.319152>.
- [4] Anderson PM, Agrawal BL, Van Ness JE. Subsynchronous resonance in power systems. New York: IEEE Press; 1990.
- [5] Kundur P. Power system stability and control. New York: McGraw-Hill; 1994.
- [6] Neto OM, Macdonald DC. Analysis of subsynchronous resonance in a multimachine power system using series compensation. Int J Elect Power Energy Syst 2006; 28 (8): 565-9. <https://doi.org/10.1016/j.ijepes.2006.02.015>.
- [7] Martins N, Paserba JJ, Pinto JCP. Using a TCSC for line power scheduling and system oscillation damping – small signal and transient stability studies. In: Proc of IEEE PES winter meeting, vol. 2. Singapore; January 2000. pp. 1455-61. <https://doi.org/10.1109/PESW.2000.850193>.
- [8] Larsen EV, Bowler CEJ, Damsky B, Nilsson S. Benefits of thyristor controlled series compensation. CIGRE Annual Meeting, Paper No. 14/37/38-04. Paris; 1992.
- [9] Ally A, Rigby BS. The impact of closed-loop power flow control strategies on the power system stability characteristics in a single generator system. SAIEE Afr Res J 2006; 97(1): 34-42.
- [10] R. Pillay Carpanen, B.S. Rigby, "An improved SSSC-based power flow controller design method and its impact on torsional interaction", Electrical Power and Energy Systems 43 (2012) 194-209. <https://doi.org/10.1016/j.ijepes.2012.05.020>.
- [11] Paul C. Krause, Oleg Wasynczuk, Scott D. Sudhoff. Analysis of Electric Machinery and Drive Systems. 2nd edition, New York, USA: IEEE Press and Wiley India Pvt. Ltd.; 2014.